Synthesis and Characterization of SF_4 Adducts with Polycyclic Amines

Nathan Kostiuk,[†,‡] *James T. Goettel,* [†,‡] *and Michael Gerken**[†,‡]

[†]Canadian Centre for Research in Advanced Fluorine Technologies, University of Lethbridge, 4401 University Drive W, Lethbridge, AB, CA T1K 3M4

[‡]Department of Chemistry and Biochemistry, University of Lethbridge, 4401 University Drive W, Lethbridge, AB, CA T1K 3M4

Canadian Centre for Research in Advanced Fluorine Technologies and the Department of Chemistry and Biochemistry, University of Lethbridge, Lethbridge Alberta, T1K 3M4, Canada.
E-mail: michael.gerken@uleth.ca

ABSTRACT: Chalcogen bonding interactions of SF_4 with the polycyclic amines DABCO ($C_6H_{12}N_2$) and HMTA ($C_6H_{12}N_4$) were studied by low-temperature Raman spectroscopy and X-ray crystallography, revealing the 2:1 adducts $C_6H_{12}N_2 \cdot 2SF_4$ and $C_6H_{12}N_4 \cdot 2SF_4$ obtained from SF_4 solvent. In $C_6H_{12}N_2 \cdot 2SF_4$, sulfur in each SF_4 molecule is pentacoordinate with each SF_4 coordinated by a single amine group, whereas $C_6H_{12}N_4 \cdot 2SF_4$ forms a one-dimensional coordination polymer with three of the four nitrogen atoms in HTMA exhibiting N---S chalcogen-bonds: one terminal N---SF_4 and one experimentally unprecedented bridging N---(SF_4)---N moiety. Solvolysis of $C_6H_{12}N_2 \cdot 2SF_4$ by HF yielded crystals of $[C_6H_{12}N_2H]^+{}_2F^-[SF_5]^- \cdot 6SF_4$, in which SF_4 acts as a chalcogen bond donor towards N as well as F. Solvolysis of $C_6H_{12}N_4 \cdot 2SF_4$ resulted in the formation of the mono-protonated HMTA salt $[C_6H_{12}N_4H]^+[HF_2]^- \cdot SF_4$. Excess HF also led to isolation of mono-protonated HTMA, as seen in the crystal structure of the $[C_6H_{12}N_4H]^+[H_2F_3]^- \cdot HF$ salt. The reaction of bicyclic, monobasic quinuclidine with SF_4 and HF gave $[C_7H_{13}NH]^+F^- \cdot 3.5SF_4$, which contains N–H---$F^-$---$SF_4$ interactions, as well as an interstitial, disordered SF_4 molecule.

INTRODUCTION

Sulfur tetrafluoride has been of interest to chemists for fundamental geometry considerations, as well as for applications as a reagent in synthetic organic and inorganic chemistry.[1,2] In reactions with strong Lewis acids, such as SbF_5, SF_4 acts as a fluoride-ion donor, yielding SF_3^+ salts.[3] Its chemistry as a fluoride-ion acceptor had been well established towards 'naked' fluorides sources.[4] The interaction between SF_4 and organic Lewis-basic functionalities is more difficult to study experimentally because of the weakness and lability of donor---S chalcogen bonding. More recently, the Lewis acidity of SF_4 towards nitrogen bases (triethylamine, pyridine, and pyridine derivatives)[5,6] and oxygen bases (THF, cyclopentanone, and dimethoxyethane)[7] has been conclusively proven by low-temperature Raman spectroscopic and X-ray crystallographic characterization. Whereas the studied nitrogen bases were found to form a single N---S chalcogen bond per SF_4 molecule, oxygen bases formed two O---S chalcogen bonds to SF_4 in adducts in the solid state. The latter observation is in line with the presence of two σ-holes on SF_4, opposite the equatorial S–F bonds, that can interact with two donor groups.[8] The N---S chalcogen bonds have been shown to be sensitive towards solvolysis by HF, yielding the protonated nitrogen-base and fluoride, which can interact with SF_4, exhibiting a range of bonding modalities.[9]

Chalcogen bonding interactions have attracted increasing interest for applications in synthesis, catalysis, anion recognition and crystal engineering.[10] Sulfur compounds are much weaker chalcogen-bond donors than those of selenium and tellurium, rendering S---A (A = chalcogen-bond acceptor) interactions difficult to study. Nevertheless, S---A chalcogen bonding has been implicated in processes such as protein folding.[11] As a stable binary sulfur compound, SF_4 can act as a model compound to investigate chalcogen bonding in the solid state, because the

strongly electron withdrawing fluorine atoms in SF_4 results in two σ-holes on sulfur that can interact with Lewis bases.[8]

Sulfur tetrafluoride forms low-temperature stable (< −40 °C) solid 1:1 adducts with nitrogen bases that have BF_3 affinity values as low as 98 kJ mol^{-1} (DMAP: 152; $N(C_2H_5)_3$: 136; 4-$NC_5H_4CH_3$: 134; NC_5H_5: 128; 2,6-$NC_5H_3(CH_3)_2$: 98 kJ mol^{-1}).[12] The present study investigates whether SF_4 behaves as a single or double chalcogen-bond donor towards polycyclic amines and if SF_4 can be trapped by organic bases at temperatures closer to ambient temperatures. The bicyclic amines DABCO (1,4-diazabicylco[2.2.2]octane) and quinuclidine, with BF_3 affinity values of 143 and 150 kJ mol^{-1}, respectively, are good candidates due to their strong Lewis basicity. Tetra-basic HMTA (hexamethylenetetramine) is also included in the study in order to investigate the number of N---S chalcogen bonds that HMTA can achieve.

RESULTS AND DISCUSSION

Synthesis and Properties of Adducts of SF_4 with Polycyclic Amines. The bicyclic diamine DABCO is soluble in SF_4 close to room temperature and reacts with excess SF_4 yielding the 1:2 adduct $C_6H_{12}N_2{\cdot}2SF_4$ (Eq. 1), in which both amine groups of one DABCO molecule form chalcogen bonds to separate SF_4 molecules. At low temperature, colourless solids precipitated. Rapid cooling to −78 °C and removal of volatiles at that temperature resulted in incorporation of additional non-adducted SF_4, in spite of a melting point of −121 °C for SF_4, as evidenced by low-temperature Raman spectroscopy. The SF_4 is presumably trapped in the solid by weak F---SF_4 chalcogen bonds. Prolonged pumping at −78 °C (> 1h) yielded the 1:2 adduct. Crystals of $C_6H_{12}N_2{\cdot}2SF_4$ grew from excess SF_4 at −20 °C and could be isolated by removal of volatiles at *ca.* −80 °C. Surprisingly, SF_4 is not as readily lost from this adduct under dynamic vacuum as observed

for the previously studied SF_4 adducts with N-bases, where complete loss of SF_4 was observed above −40 °C.[5,6] In one instance, pumping at room temperature for less than 15 min yielded a solid that still contained strongly adducted SF_4 based on its Raman spectrum. Prolonged pumping at room temperature (ca. 30 min) resulted in recovery of non-adducted DABCO.

$$C_6H_{12}N_2 + 2SF_4 \rightarrow \quad C_6H_{12}N_2{\cdot}2SF_4 \qquad (1)$$

The reaction of HMTA with excess SF_4 also yields a colourless 1:2 adduct, i.e., $C_6H_{12}N_4{\cdot}2SF_4$ (Eq 2). Although four amine functionalities are present per HMTA molecule, no evidence for the incorporation of additional aliquots of SF_4 in the solid adduct was found.

$$C_6H_{12}N_4 + 2SF_4 \rightarrow \quad C_6H_{12}N_4{\cdot}2SF_4 \qquad (2)$$

As previously observed for SF_4-N-base adducts,[9] the S---N chalcogen bond can easily be solvolyzed by HF. Leaving a sample of $C_6H_{12}N_4{\cdot}2SF_4$ with excess SF_4 in a cold bath at −80 °C for ca. 2 months, resulted in solvolysis of the adduct by HF and formation of single crystals of $[C_6H_{12}N_2H]^+{}_2F^-[SF_5]^-{\cdot}6SF_4$ (Eq 3). Apparently water slowly diffused through the FEP sample tube and hydrolysed SF_4, generating HF. This salt still contains one S---N chalcogen bond between DABCO and SF_4 and has additional SF_4 molecules incorporated in the crystal structure (vide infra). Solvolysis of the $C_6H_{12}N_4{\cdot}2SF_4$ using two aliquots of HF produced the singly protonated HMTA fluoride salt $[C_6H_{12}N_4H]^+[HF_2]^-{\cdot}SF_4$ (Eq 4), in which the second HF molecules combined with F^- to form the HF_2^- anion, which is hydrogen-bonded to the protonated amine group. Even with excess HF, only the singly protonated HMTA was obtained, as evidenced by the crystal structure of $[C_6H_{12}N_4H]^+[H_2F_3]^-{\cdot}HF$ (vide infra).

$$2\ C_6H_{12}N_2{\cdot}2SF_4 + 3SF_4 + 2HF \rightarrow [C_6H_{12}N_2H]^+{}_2F^-[SF_5]^-{\cdot}6SF_4 \qquad (3)$$

$$C_6H_{12}N_4{\cdot}2SF_4 + 2HF \rightarrow [C_6H_{12}N_4H]^+[HF_2]^-{\cdot}SF_4 + SF_4 \qquad (4)$$

Bicyclic quinuclidine ($C_7H_{13}N$) has, in contrast to DABCO, only one amine group available to react with SF_4. Unfortunately, no conclusive evidence could be obtained for a $C_7H_{13}N{\cdot}SF_4$ adducts, because reaction products did not give crystals suitable for X-ray crystallography and fluorescence caused low-temperature Raman spectroscopy to be inconclusive. Introduction of stoichiometric amounts of HF, generated via controlled hydrolysis of excess SF_4, gave crystals of the HF solvolysis product $[C_7H_{13}NH]^+F^-{\cdot}3.5SF_4$ from excess SF_4 solvent upon removal of volatiles at −90 °C.

$$C_7H_{13}N + 3.5\ SF_4 + HF \rightarrow [C_7H_{13}NH]^+F^-{\cdot}3.5SF_4 \qquad (5)$$

Because all of the SF_4-containing compounds are only stable below ambient temperature, handling at low temperature was necessary during isolation and characterization.

Crystallography. The two 1:2 adducts of DABCO and HMTA with SF_4, $C_6H_{12}N_2{\cdot}2SF_4$ and $C_6H_{12}N_4{\cdot}2SF_4$, respectively, were characterized by single-crystal X-ray diffraction. Selected metric parameters are given in Table 1, whereas crystal data collection parameters are listed in Table S1 in the Supporting Information.

The $C_6H_{12}N_2{\cdot}2SF_4$ adduct crystallizes in the monoclinic space group $P2_1/c$ with one adduct molecule in the assymmetric unit (Figure 1). Both nitrogen atoms of DABCO form chalcogen bonds to two different SF_4 molecules with similar S---N distances (2.362(4) and 2.337(4) Å), which are comparable to that in $Et_3N{\cdot}SF_4$ (2.3844(19) Å).[5] The geometries of the N---SF_4 moieties are square pyramidal, and the metric parameters of the SF_4 moieties in the DABCO adduct are similar to that of the NEt_3 adduct, with the apical S−F bonds that are *cis* to the S---N chalcogen bond and *trans* to the lone pair being the shortest (S(1)−F(1): 1.561(3) and S(2)−F(5): 1.574(3) Å), followed by the S−F bonds *trans* to the S---N chalcogen bond (S(1)−F(2): 1.596(3) and

S(2)−F(6): 1.595(3) Å). The two S−F bonds *cis* to the S---N dative bonds, and *trans* to each other, which correspond to the axial bonds in free SF_4, are substantially longer (1.684(3) to 1.697(3) Å), in agreement with the other structurally characterized SF_4-Lewis base adducts.[5,6] The DABCO moiety exhibits a small distortion from D_{3h} symmetry with a slight twisting (N−C−C−N torsion angles: 4.2(3), 4.9(3), and 5.1(3)°). Such twisting has been observed for other DABCO compounds, such as the DABCO·$2H_2O_2$.[13] The crystal structure of neat DABCO, on the other hand, showed a non-twisted conformation, based on neutron diffraction data.[14]

The $C_6H_{12}N_4$·$2SF_4$ adduct, which crystallized in the orthorhombic *Pnma* space group, is a 1-dimensional coordination polymer in the solid state, containing one bridging SF_4 moiety that forms two chalcogen bonds to nitrogen atoms of two adjacent HMTA molecules (Figure 1). The second SF_4 molecule accepts a dative bond from one nitrogen atom (N(2)), leaving the fourth amine nitrogen atom (N(3)) of HMTA uncoordinated. The HMTA molecule is bisected by a crystallographic mirror plane with N(2) and N(3) located in that plane of symmetry. As a consequence of the mirror symmetry, the terminally coordinated SF_4 molecule (coordinated to N(2)) is orientationally disordered (see Fig. S1). The S(2)---N(2) distance (2.460(3) Å) is significantly longer than those in the DABCO·$2SF_4$ adduct, indicating the weaker Lewis basicity of HMTA, as expected from the closer proximity of the amine functionalities, *i.e.*, CH_2 versus C_2H_4 spacers. The equatorial F−S−F angle of the bridging SF_4 molecule is also bisected by a mirror plane, which imposes the symmetric nature of the SF_4 bridge. The S(1)---N(1) distances (2.774(3) Å) are markedly longer than that to the terminally coordinated SF_4. The terminal coordination of the SF_4 by N(2) is the expected, previously observed coordination type for nitrogen bases, whereas the presence of two chalcogen bonds to the one SF_4 is experimentally unprecedented for nitrogen-bases. This coordination mode, however, has been observed for less

Lewis-basic oxygen-bases,[7] and N---S---N double chalcogen bonds have been computationally predicted for SF_4 and ammonia.[8b] Apparently the terminal coordination of one SF_4, reduces the Lewis basicity of HMTA sufficiently, so that the Lewis basicity of the second amine functionality resembles that of an oxygen base, leading to dicoordination to SF_4. The decreased Lewis basicity parallels the significant reduction of in Bronsted basicity ($pK_{b,1} = 9.11$; $pK_{b,2} = 15.7$).[15]

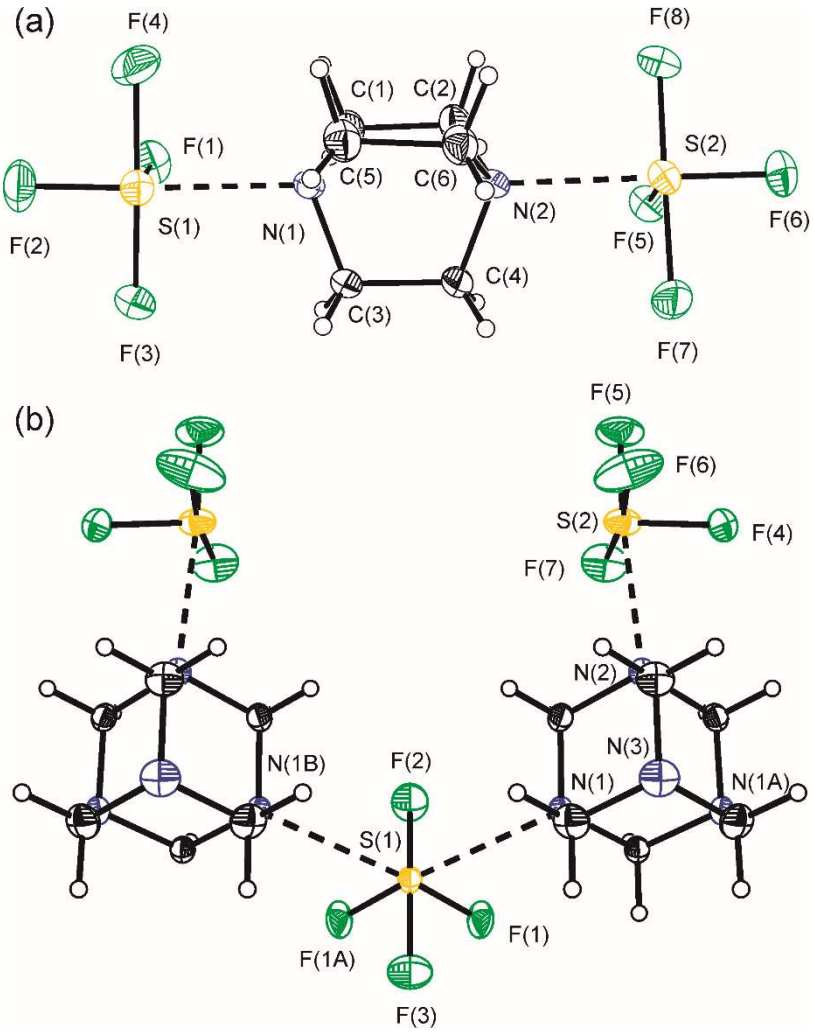

Figure 1. Thermal ellipsoid plot of the (a) $C_6H_{12}N_2 \cdot 2SF_4$ and (b) $C_6H_{12}N_4 \cdot 2SF_4$ adducts. Only one orientation of the disordered terminally coordinated SF_4 in $C_6H_{12}N_4 \cdot 2SF_4$ is shown. Thermal ellipsoids are drawn at the 50% probability level.

Table 1. Selected Bond Lengths (Å), Contacts (Å), and Angles (°) of $C_6H_{12}N_2{\cdot}2SF_4$ and $C_6H_{12}N_4{\cdot}2SF_4$.

$C_6H_{12}N_2{\cdot}2SF_4$			
Bond Lengths and Contacts, Å		Bond Angles, deg.	
S(1)–F(1)/S(2)–F(5)	1.561(3)/1.574(3)	F(1)–S(1)–F(2)/ F(5)–S(2)–F(6)	92.66(11)/92.27(9)
S(1)–F(2)/S(2)–F(6)	1.596(3)/1.595(3)	F(3)–S(1)–F(4)/ F(7)–S(2)–F(8)	171.01(11)/170.86(10)
S(1)–F(3)/S(2)–F(7)	1.685(3)/1.684(3)	F(1)–S(1)–N(1)/ F(5)–S(2)–N(2)	82.22(9)/81.07(8)
S(1)–F(4)/S(2)–F(8)	1.685(3)/1.697(3)	F(2)–S(1)–N(1)/ F(5)–S(2)–N(2)	174.80(9)/173.26(9)
S(1)---N(1)/S(2)---N(2)	2.362(4)/2.337(4)		
$C_6H_{12}N_4{\cdot}2SF_4$			
Bond Lengths and Contacts, Å		Bond Angles, deg.	
S(1)–F(1)	1.5647(16)	F(1)–S(1)–F(1A)^{i}	94.50(12)
S(1)–F(1A)^{i}	1.5648(16)	F(2)–S(1)–F(3)	172.50(10)
S(1)–F(2)	1.683(2)	F(1)–S(1)–N(1)	76.13(9)
S(1)–F(3)	1.676(2)	F(1A)–S(1)–N(1)	169.99(5)
S(1)---N(1)/S(1)---N(1A)^{i}	2.774(3)/2774(3)	N(1)---S(1)---N(1A)^{i}	112.99(10)
S(2)–F(4)	1.543(3)	F(4)–S(2)–F(5)	95.0(5)
S(2)–F(5)	1.578(3)	F(6)–S(2)–F(7)	172.1(3)
S(2)–F(6)	1.670(3)	F(4)–S(2)–N(2)	79.72(10)
S(2)–F(7)	1.626(3)	F(5)–S(2)–N(2)	173.4(4)
S(2)---N(2)	2.460(3)		

Symmetry codes: (i) x, –y–1/2, z.

The solvolysis products of the 1:2 adducts of DABCO and HMTA with SF_4, $[C_6H_{12}N_2H]^+{}_2F^-[SF_5]^-{\cdot}6SF_4$ and $[C_6H_{12}N_4H]^+[HF_2]^-{\cdot}SF_4$, respectively, were characterized by single-crystal X-ray diffraction. In addition, crystal strutures of $[C_6H_{12}N_4H]^+[H_2F_3]^-{\cdot}HF$ and $[C_7H_{13}NH]^+F^-{\cdot}3.5SF_4$ were obtained. Selected metric parameters are given in Table 2, whereas crystal data collection parameters are listed in Table S2 in the Supporting Information.

The solvolysis product of $C_6H_{12}N_2{\cdot}2SF_4$, $[C_6H_{12}N_2H]^+{}_2F^-[SF_5]^-{\cdot}6SF_4$, crystallizes from excess SF_4 in the orthorhombic *Pbca* space group and contains two crystallographically unique, singly protonated DABCO molecules with the unprotonated nitrogens coordinated to SF_4. These two singly protonated DABCO molecules hydrogen-bond to the same fluoride anion, which, in

turn, forms F---S chalcogen bonds to two SF_4 molecules, forming the $[(F_4S{-}{-}{-}NC_6H_{12}NH)_2F(SF_4)_2]^+$ cationic moiety (Figure 2a). A similar motif has been observed in the protonated 2,6-dimethylpyridine structure $[HNC_5H_3(CH_3)_2]^+_2[SF_5]^-F^-{\cdot}SF_4$.[6] The F---S chalcogen bonds to two SF_4 molecules (2.662(5) and 2.641(4) Å) in the DABCO structure are in contrast to the 2,6-dimethylpyridinium structure, in which the hydrogen-bonded fluoride anion coordinates significantly stronger towards one SF_4 molecule (F---S: 2.5116(12) Å). As in the 2,6-dimethylpyridinium structure, the remaining fluoride anion is left sufficiently 'naked' to combine with SF_4 to form the SF_5^- anion. Two equatorial fluorine atoms of the SF_5^- anion form weak S---F contacts to one of the adducted SF_4 molecules, i.e., $S(2)F_4$ (3.216(8) Å), and an additional non-adducted SF_4 molecule, i.e., $S(5)F_4$ (3.119(8) Å), which are close to the limit of the sum of the van der Waals radii (3.35 Å)[16] (Figure 2b). These two contacts keep the two basal fluorines that are *trans* to each other fixed, allowing for a rotational disorder of the SF_5^- anion about this F–S–F axis. The $S(7)F_4$ molecule exhibits an positional disorder with one axial fluorine atom acting as the pivot point; this axial fluorine atom is weakly held in place by a S---F contact (3.110(7) Å) to the $S(3)F_4$ molecule (Figure S2).

The S---N distances (2.514(5) and 2.594(5) Å) in $[C_6H_{12}N_2H]^+_2F^-[SF_5]^-{\cdot}6SF_4$ are significantly longer than those in the $C_6H_{12}N_2{\cdot}2SF_4$ adduct, as a consequence of the reduced Lewis basicity upon protonation of one amine group of DABCO. The S---N distance is closer to that in the pyridine adduct of SF_4 (2.514(2) Å) than that in the triethylamine adduct (2.3844(19) Å). The structure contains one ordered SF_4 molecule that does not have any contacts to DABCO or fluoride. The metric parameters of this SF_4 molecule are within the range of the values for solid SF_4, with a F_{eq}–S–F_{eq} of 101.2(3)°,[17] which is not contracted by any contact as in the other adducted SF_4 molecules (N---SF_4: 95.4(2) and 96.08(19)°;[5,6] F^----SF_4, 98.5(2) and 99.0(3)°).[9] This structure

exemplifies how easily SF_4 can be incorporated into the solid state at low temperature via chalcogen bonds and corroborates the Raman spectroscopic finding of facile incorporation of SF_4 into $C_6H_{12}N_2{\cdot}2SF_4$ at low temperature (vide infra). Similar incorporation of additional SF_4 molecules has been observed in the 2,6-dimethylpyridinium structure $[HNC_5H_3(CH_3)_2]^+{}_2[SF_5]^-F^-{\cdot}4SF_4$.[17]

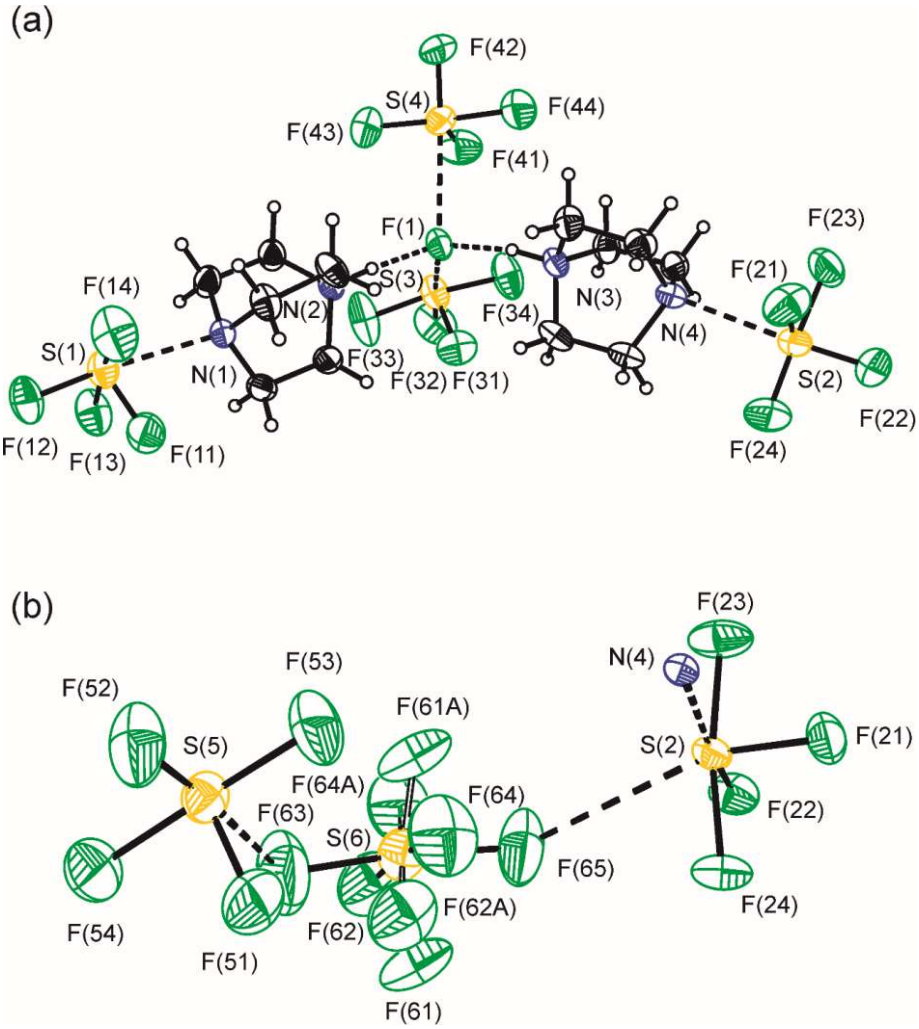

Figure 2. (a) Thermal ellipsoid plots of the $[(F_4S{-}{-}{-}NC_6H_{12}NH)_2F(SF_4)_2^+]$ cationic moiety in $[C_6H_{12}N_2H]^+{}_2F^-[SF_5]^-{\cdot}6SF_4$. Thermal ellipsoids are drawn at the 50% probability level. (b) Thermal ellipsoid plots of the interactions between the $[SF_5^-]$ anion with two SF_4 molecules in $[C_6H_{12}N_2H]^+{}_2F^-[SF_5]^-{\cdot}6SF_4$. Thermal ellipsoids are drawn at the 30% probability level.

Table 2. Selected Bond Lengths (Å), Contacts (Å), and Angles (°) of $[C_6H_{12}N_2H]^+{}_2F^-[SF_5]^-\cdot 6SF_4$, $[C_6H_{12}N_4H]^+[HF_2]^-\cdot SF_4$, $[C_6H_{12}N_4H]^+[H_2F_3]^-\cdot HF$, and $[C_7H_{13}NH^+]F^-\cdot 3.5SF_4$.

$[C_6H_{12}N_2H]^+{}_2F^-[SF_5]^-\cdot 6SF_4$			
Bond Lengths and Contacts, Å		Bond Angles, deg.	
S(1)–F(11)/S(2)–F(21)	1.539(4)/1.551(4)	F(11)–S(1)–F(12)/ F(21)–S(2)–F(22)	95.4(2)/96.08(19)
S(1)–F(12)/S(2)–F(22)	1.584(3)/1.577(4)	F(13)–S(1)–F(14)/ F(23)–S(2)–F(24)	172.76(19)/171.2(2)
S(1)–F(13)/S(2)–F(23)	1.692(4)/1.690(4)	F(11)–S(1)–N(1)/ F(21)–S(2)–N(4)	80.11(17)/80.78(16)
S(1)–F(14)/S(2)–F(24)	1.693(4)/1.669(4)	F(12)–S(1)–N(1)/ F(22)–S(2)–N(4)	175.23(16)/176.38(15)
S(1)---N(1)/S(2)---N(4)	2.514(5)/2.594(5)		
S(3)–F(31)/S(4)–F(41)	1.545(4)/1.547(4)	F(31)–S(3)–F(32)/ F(41)–S(4)–F(42)	98.5(2)/99.0(3)
S(3)–F(32)/S(4)–F(42)	1.561(4)/1.553(4)	F(33)–S(3)–F(34)/ F(43)–S(4)–F(44)	172.6(2)/168.4(3)
S(3)–F(33)/S(4)–F(43)	1.668(4)/1.686(5)	F(31)–S(3–F(1)/ F(41)–S(4)–F(1)	76.44(16)/79.32(19)
S(3)–F(34)/S(4)–F(44)	1.669(4)/1.669(5)	F(32)–S(3)–F(1)/ F(42)–S(4)–F(1)	174.88(17)/176.5(2)
S(3)---F(1)/S(4)---F(1)	2.662(5)/2.641(4)		
F(1)---N(2)/F(1)---N(3)	2.598(5)/2.613(6)		
S(5)–F(51)	1.505(5)	F(51)–S(5)–F(52)	101.2(3)
S(5)–F(52)	1.520(5)	F(53)–S(5)–F(54)	171.9(3)
S(5)–F(53)	1.656(5)		
S(5)–F(54)	1.657(5)		
$[C_6H_{12}N_4H]^+[HF_2]^-\cdot SF_4$			
Bond Lengths and Contacts, Å			Bond Angles, deg.
S(1)–F(1)	1.572(10)	F(1)–S(1)–F(1B)^{i}	98(2)
S(1)–F(1B)^{i}	1.572(10)	F(2)–S(1)–F(3)	169.4(7)
S(1)–F(2)	1.658(8)	F(1)^{i}–S(1)–N(1)	75.7(10)
S(1)–F(3)	1.668(11)	F(1)–S(1)–N(1)	169.4(8)
S(1)---N(1)	2.791(2)	N(1)---S(1)---N(1B)^{i}	108.93(9)
N(2)---F(4)	2.523(4)		
F(5)---F(4)	2.309(4)		
$[C_6H_{12}N_4H^+][H_2F_3^-]\cdot HF$			
Bond Lengths and Contacts, Å		Bond Angles, deg.	
N(4)---F(4)	2.7494(17)	F(2)---F(3)---F(4)	121.16(6)
N(4)---F(2)^{ii}	2.808(17)		
N(1)---F(1)	2.5220(18)		
F(2)---F(3)	2.3115(17)		
F(4)---F(3)	2.2968(17)		

$[C_7H_{13}NH]^+F^-\cdot 3.5SF_4$			
Bond Lengths and Contacts, Å		Bond Angles, deg.	
S(1)–F(1)	1.5415(18)	F(1)–S(1)–F(2)	97.54(11)
S(1)–F(2)	1.551(2)	F(3)–S(1)–F(4)	171.54(12)
S(1)–F(3)	1.654(2)	F(1)–S(1)---F(5)	78.62(8)
S(1)–F(4)	1.677(2)	F(2)–S(1)---F(5)	174.20(10)
S(1)---F(5)	2.4945(13)		

Symmetry codes: (i) x, −y+5/2, z; (ii) −x+1/2, y+1/2, −z+3/2.

The solvolysis product of $C_6H_{12}N_4\cdot 2SF_4$, $[C_6H_{12}N_4H]^+[HF_2]^-\cdot SF_4$, crystallizes in the *Pnma* space group and contains a singly protonated HMTA. The terminally, more strongly coordinated SF_4 is displaced by a proton that is hydrogen bonded to an HF_2^- anion (Figure 3). The difference in size of the thermal ellipsoids of the two fluorine atoms in HF_2^- reflect the more tightly held hydrogen-bonded fluoride compared to the terminal fluorine atom. The bridging SF_4 molecule remains in place, maintaining the 1-dimensional coordination polymer motif. In comparison to the $C_6H_{12}N_4\cdot 2SF_4$ adduct, the bridging S---N distances in this salt is elongated (2.791(2) versus 2.774(3) Å). The longer chalcogen bonds provide the bridging SF_4 molecule with more rotational freedom, allowing for disorder (Figure 3). In a sample with excess of HF, crystals of $[C_6H_{12}N_4H]^+[H_2F_3]^-\cdot HF$ were obtained, where still only one amine group in HMTA is protonated and a second is hydrogen-bonded to HF (Figure 4), which is in agreement with dramatic decrease in the Bronsted basicity of protonated HTMA compared to neutral HTMA. The $H_2F_3^-$ counter anion exhibits a bent geometry with F---F distances of 2.2968(17) and 2.3115(17) Å. This anion has previously been observed in the structures of $[N(CH_3)_4][H_2F_3]$ (F---F: 2.3218(5) and 2.3284(5) Å) and $Cs[H_2F_3]$ (F---F: 2.30(1) and 2.34(1) Å).[18]

While no structural information could be obtained for a potential quinuclidine adduct of SF_4, its solvolysis product using one aliquot of HF crystallized from SF_4 as $[C_7H_{13}NH]^+F^-\cdot 3.5SF_4$. The structure revealed the expected protonated quinuclidine $C_7H_{13}NH^+$ cation, which is hydrogen-

bonded to fluoride. The molecular C_3 axis of $C_7H_{13}NH^+$ coincides with a crystallographic C_3 rotational axis, along which the fluoride ion is located. Imposed by crystallographic symmetry, the fluoride ion coordinates towards three symmetry-related SF_4 molecules (F---S: 2.4945(13) Å). The axial fluorine atoms of SF_4 form weak F---S contact (3.075(2) Å), resulting in an unprecedented structural unit comprising six SF_4 molecules and two $[C_7H_{13}NH]^+F^-$ ion pairs (Figure 5), which are aligned along the *z*-axis. The packing of these $(C_7H_{13}NH^+---F^-)_2 \cdot 6SF_4$ units leaves a cavity that is occupied by one fully rotationally disordered SF_4 molecule located on a 3 2 symmetry site (Figure S3), resulting in alternating $(C_7H_{13}NH^+---F^-)_2 \cdot 6SF_4$ and SF_4 units along the *z*-axis. The nature of the interstitial molecule was confirmed by the SQUEEZE program within PLATON that gave the number of electrons present in the cavity.[19]

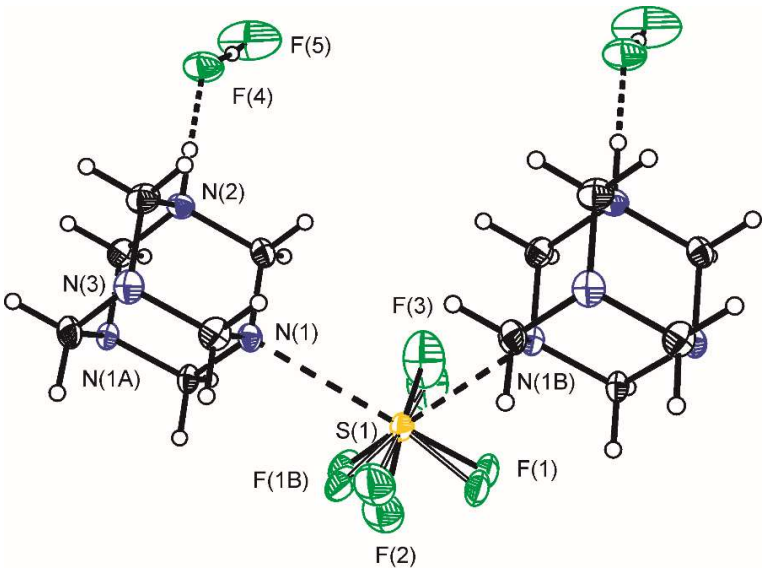

Figure 3. Thermal ellipsoid plots of the $[C_6H_{12}N_4H]^+[HF_2]^- \cdot SF_4$ structure. Thermal ellipsoids are drawn at the 50% probability level.

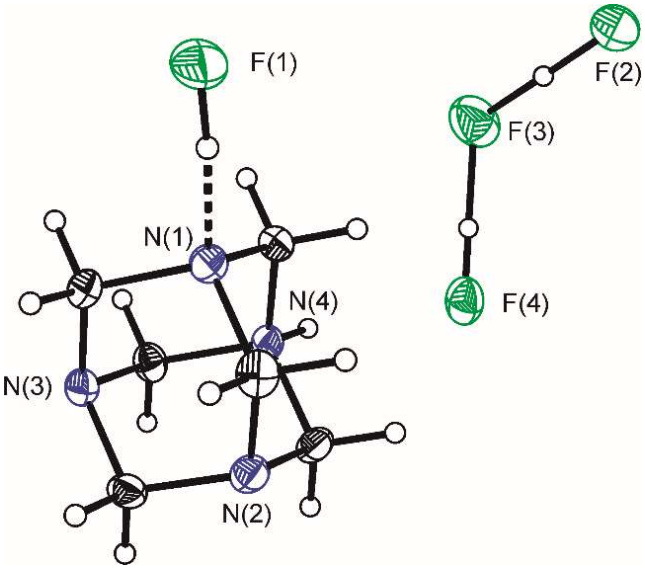

Figure 4. Thermal ellipsoid plots of the $[C_6H_{12}N_4H]^+[H_2F_3]^-\cdot HF$ structure. Thermal ellipsoids are drawn at the 50% probability level.

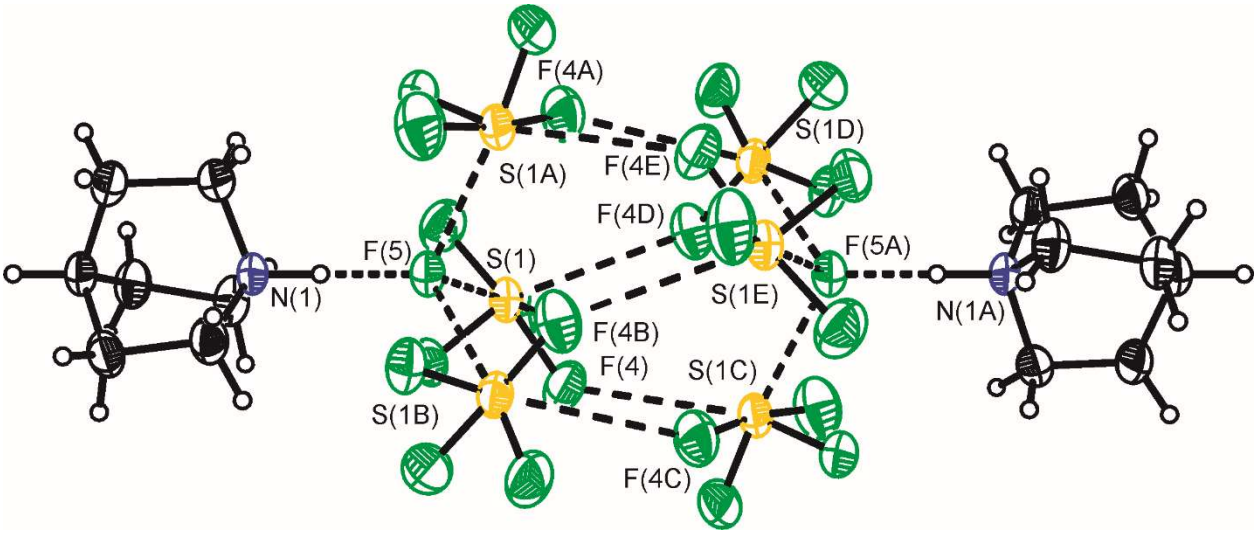

Figure 5. Thermal ellipsoid plots of the $(C_7H_{13}NH^+\text{---}F^-)_2\cdot 6SF_4$ structural unit in the $[C_7H_{13}NH]^+F^-\cdot 3.5SF_4$ structure. The disordered interstitial SF_4 molecule is not shown. Thermal ellipsoids are drawn at the 50% probability level.

Raman Spectroscopy. Raman spectra of $C_6H_{12}N_2{\cdot}2SF_4$ and $[C_6H_{12}N_2H]^+{}_2F^-[SF_5]^-{\cdot}nSF_4$ were obtained at −100 °C. Their vibrational frequencies are listed in Table S3 together with those of neat DABCO and tentative assignments. The assignments of Raman bands is based on that for DABCO and its mono- and di-protonated forms in aqueous solutions,[20] as well as the assignments of SF_4 bands of previously reported adducts.

The Raman spectrum of $C_6H_{12}N_2{\cdot}2SF_4$ (Figure 6) was recorded on a solid sample after pumping off excess SF_4 at −76 °C for approximately 4.5 hours. Only small signals attributed to non-adducted, excess SF_4 were observed. The Raman spectrum for $C_6H_{12}N_2{\cdot}2SF_4$ contains characteristic signals for adducted SF_4 in addition to those for the DABCO moiety. Bands in the S−F stretching region were attributed to $\nu(SF_{apical})$ (836 and 821 cm^{-1}), $\nu(SF_{trans})$ (728 cm^{-1}), $\nu_{as}(SF_{2,cis})$ (647 cm^{-1}), and $\nu_s(SF_{2,cis})$ (495 cm^{-1}). The vibrational frequencies of the SF_4 moieties lie in the range of the corresponding frequencies observed for the SF_4 adducts with pyridine and its derivatives as well as that with $N(C_2H_5)_3$.[5,6] For example, the apical S−F stretching mode of the square pyramidal NSF_4 moiety lies between that of $C_5H_5N{\bullet}SF_4$ (852 cm^{-1}) and $(CH_3)_2NC_5H_4N{\bullet}SF_4$ (791 cm^{-1}), most similar to those of $(C_2H_5)_3N{\bullet}SF_4$ (826, 816 cm^{-1}). This is consistent with the crystal structure of $C_6H_{12}N_2{\cdot}2SF_4$ that shows S---N bond lengths similar to the S---N distances in $(C_2H_5)_3N{\bullet}SF_4$ (*vide supra*). Raman bands attributed to the DABCO moiety exhibit slight shifts upon adduct formation. Most indicative is the shift of the strong Raman signal (ν(CC)/$\omega(CH_2)$ mode) at 971 cm^{-1} in solid DABCO to 990 cm^{-1} in the 1:2 adduct; such a shift was also observed upon protonation.[20]

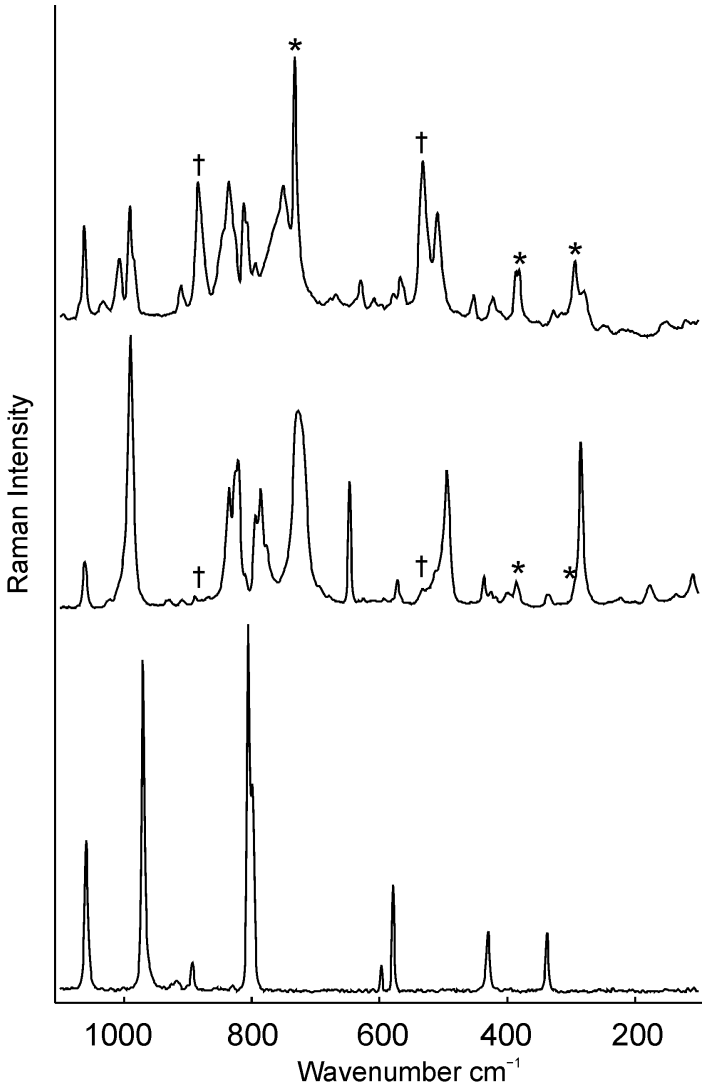

Figure 6. Raman spectra of DABCO (lower trace), $C_6H_{12}N_2{\cdot}2SF_4$ (middle trace), and $[C_6H_{12}N_2H]^+{}_2F^-[SF_5]^-{\cdot}nSF_4$ (upper trace) recorded at room-temperature, −100 °C, and −100 °C, respectively. Asterisks (*) and dagger (†) denote bands arising from the FEP sample tube and non-adducted SF_4, respectively.

The Raman spectrum was recorded on a white solid obtained from the reaction of DABCO, 2 HF and excess SF_4, after removal of volatiles at low temperature. The spectrum is consistent with the formula $[C_6H_{12}N_2H]^+{}_2F^-[SF_5]^-{\cdot}nSF_4$, similar to the composition of the crystal structure (vide

supra), although the exact content of non-adducted SF_4 in the bulk solid cannot be ascertained. Although two equivalents of HF were present, DABCO was only singly protonated, consistent with the dramatic reduction of basicity upon mono-protonation ($pK_{b,1}$ = 5.2, $pK_{b,2}$ = 11.0).[21] The Raman spectrum features bands that are indicative of protonated DABCO, $[C_6H_{12}N_2H]^+$, at 1008 and 608 cm^{-1} arising from skeletal deformation caused by asymmetric protonation of one amine group.[20] As in $C_6H_{12}N_2{\cdot}2SF_4$, the strong Raman band associated with the ν(CC)/ω(CH_2) mode is shifted to 992 cm^{-1} compared to solid DABCO. Two sets of Raman signals attributable to SF_4 are observed, i.e., adducted SF_4, with the $\nu(SF_{apical})$ band at 836 cm^{-1}, and non-adducted SF_4, with the $\nu_s(SF_{2,eq})$ band at 884 cm^{-1}. The bands assigned to non-adducted SF_4 are in good agreement with those found in $[HNC_5H_3(CH_3)_2]^+{}_2F^-\cdots SF_4[SF_5]^-{\bullet}3SF_4$[17] and in solid SF_4.[22] Bands characteristic of the $[SF_5]^-$ anion are present between 800 and 250 cm^{-1}, most notably at 578, 452, 422 and 250 cm^{-1} where the signals are well differentiated from SF_4 signals.

Raman spectra of solid samples of $C_6H_{12}N_4{\cdot}2SF_4$ and $[C_6H_{12}N_4H]^+[HF_2]^-{\cdot}SF_4$ recorded at −100 °C are shown in Figure 7 and vibrational frequencies are listed in Table S4. The tentative assignments for bands attributed to the HMTA moiety are based on the vibrational assignments by Bertie and Solinas.[23] The Raman spectrum of the 1:2 adduct $C_6H_{12}N_4{\cdot}2SF_4$ contains bands that are attributable to the HMTA moiety and adducted SF_4. The shifts of the vibrational frequencies of the SF_4 moiety in the adduct compared to neat SF_4 are in good agreement with those observed for adducts with N-bases. For example, the highest frequency S−F bands at 849 and 843 cm^{-1} are between those observed for $SF_4{\cdot}py$ (852 cm^{-1})[6] and $SF_4{\cdot}NEt_3$ (826, 816 cm^{-1}).[5] The observation of splittings of most bands associated with SF_4 group corroborates the presence of two types of adducted SF_4 in the crystal structure of $C_6H_{12}N_4{\cdot}2SF_4$, i.e., terminal and bridging. Based on the observation that bands of dicoordinated SF_4 (in adducts with O-bases) exhibit a smaller shift from

those of free SF_4 than the bands of mono-coordinated SF_4 (in adducts with N-bases), tentative assignments have been made for both types of adducted SF_4.

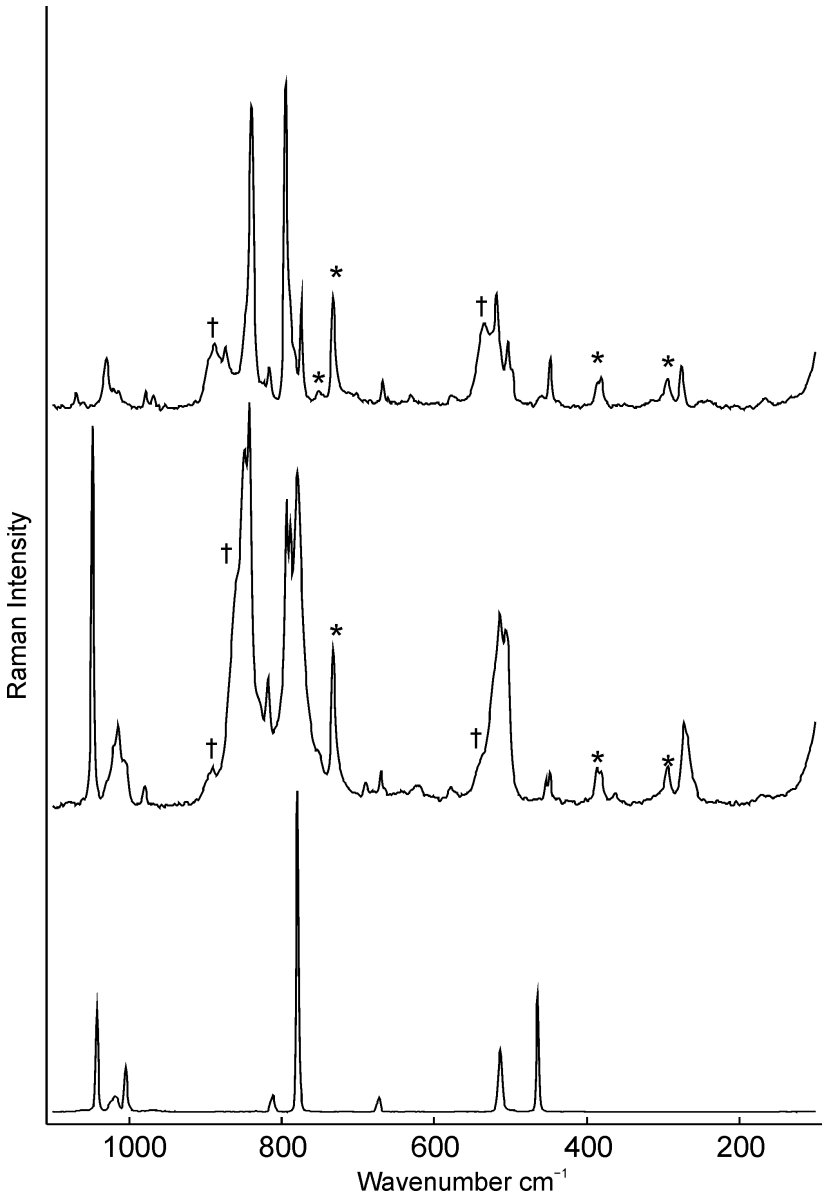

Figure 7. Raman spectra of HMTA (lower trace), $C_6H_{12}N_4 \cdot 2SF_4$ (middle trace), and $[C_6H_{12}N_4H]^+[HF_2]^- \cdot SF_4$ (upper trace) recorded at room-temperature, −100 °C, and −100 °C, respectively. Asterisks (*) and dagger (†) denote bands arising from the FEP sample tube and free SF_4, respectively.

The Raman spectrum of the solid product of the solvolysis product $[C_6H_{12}N_4H]^+[HF_2]^-\cdot SF_4$, shows only one set of bands for adducted SF_4, i.e., bridging, di-coordinated SF_4, which corroborates the observation of the absence of the terminal SF_4. Significantly intense signals for excess SF_4 (889 cm^{-1}), as well as weakly associated SF_4 (874 cm^{-1}), are observed although the sample was a solid at −100 °C. This nicely shows the facile incorporation of SF_4 in solid samples presumably via chalcogen bonding. The band at 874 cm^{-1} is close to that observed for SF_4 in the layers of $[HNC_5H_3(CH_3)_2]^+{}_2F^-\cdots SF_4[SF_5]^-\bullet 3SF_4$. The band at 578 cm^{-1} is attributed to bifluoride. The presence of such a band in the spectrum of the bulk adduct without solvolysis, indicates that some moisture had led to accidental hydrolysis.

CONCLUSIONS

Polycyclic amines such as DABCO and HMTA were shown to form 1:2 Lewis acid base adducts with SF_4, containing N---S chalcogen bonding interactions. While dibasic DABCO coordinates to two SF_4 molecules in a terminal fashion, tetrabasic HMTA coordinates to one terminal SF_4 molecule and to a second one in a bridging fashion. The observation of two N---S chalcogen bonds to one SF_4 molecule is experimentally unprecedented and is similar to the bonding in adducts with O-bases. These double chalcogen bonds utilize both of the two σ-holes present on sulfur in SF_4. Crystal structures of solvolysis products of the DABCO adduct, $C_6H_{12}N_2\bullet 2SF_4$, and the salt of protonated quinuclidine, $[C_7H_{13}NH]^+F^-\cdot 3.5SF_4$, show the facile incorporation of non-adducted SF_4 in the solid state. In addition, the observation that some SF_4 could be retained in solid mixtures with DABCO at temperatures closer to room temperature shows promise that some structural motives could enable the capture of SF_4 at room temperature.

EXPERIMENTAL SECTION

CAUTION: Sulfur tetrafluoride and HF are highly corrosive and toxic and need to be handled with the necessary precautions. Reactions with SF_4 above its boiling point (−38 °C) in sealed reaction vessels result in high pressures.

All distillations of SF_4 were performed on a metal vacuum system constructed of nickel and steel. Dichloromethane was vacuum distilled using a Pyrex glass vacuum line fitted with J-Young valves. Reactors were crafted from fluorinated ethylene-propylene copolymer tubing and fitted with Kel-F valves. All reaction vessels were rigorously dried by dynamic vacuum overnight followed by treatment with 1 atm of F_2 gas overnight.

Sulfur tetrafluoride (Ozark-Mahoning Co.) was purified by passing through activated charcoal. Trace amounts of sulfur hexafluoride and thionyl fluoride were present in the SF_4. 1,4-Diazabicyclo[2.2.2]octane (DABCO), 1-azabicyclo[2.2.2]octane (quinuclidine), and hexamethylenetetramine (HMTA) were used as received. Dichloromethane was dispensed from a dry solvent purification system (MBraun) and stored over 4A molecular sieves prior to being vacuum distilled.

Preparation of $C_6H_{12}N_2{\cdot}2SF_4$. 1,4-Diazabicyclo[2.2.2]octane (DABCO) (0.011 g, 0.098 mmol) was loaded into a ¼-in. O.D. FEP reactor. Sulfur tetrafluoride (0.100 g, 0.93 mmol) was distilled by vacuum at −197 °C and, after warming to −70 °C, a white solid formed as a suspension in liquid SF_4. Upon warming to room temperature followed by cooling to −20 °C, clear, colourless crystals of $C_6H_{12}N_2{\cdot}2SF_4$ formed. These crystals were characterized by X-ray crystallography.

Preparation of $[C_6H_{12}N_2H]^+{}_2F^-[SF_5]^-\cdot 4SF_4$. Inside of a nitrogen atmosphere dry box, 1,4-diazabicyclo[2.2.2]octane (DABCO) (0.012 g, 0.11 mmol) was loaded into a ¼-in. O.D. FEP reactor. An excess of sulfur tetrafluoride (0.140 g, 1.30 mmol) was vacuum distilled upon the solid at –197 °C, upon agitation at –50 °C the mixture reacted vigorously. Excess SF_4 was removed by vacuum at –80 °C. The reactor was stored at –80 °C where it was slowly hydrolysed over 2 months, producing clear colourless crystals of $[C_6H_{12}N_2H]^+{}_2F^-[SF_5]^-\cdot 4SF_4$.

Preparation of $[C_7H_{13}NH]^+F^-\cdot 3.5SF_4$. 1-Azabicyclo[2.2.2]octane (0.010 g, 0.090 mmol) was loaded into a ¼-in. O.D. FEP reactor using a nitrogen atmosphere dry-box. Sulfur tetrafluoride (0.284 g, 2.63 mmol) was distilled into the reactor at –197 °C. Upon warming to ca. 0 °C, a vigorous reaction occurred yielding a clear yellow solution. The solution was stored at –75 °C for one hour, upon which crystals of $[C_7H_{13}NH]^+F^-\cdot 3.5SF_4$ grew. Excess SF_4 was removed by vacuum at –85 °C directly before the crystals were characterized by X-ray crystallography.

Preparation of $[C_6H_{12}N_4H]^+[HF_2]^-\cdot SF_4$. Inside of a nitrogen atmosphere dry-box, hexamethylenetetramine (HMTA) (6.0 mg, 43 μmol) was added to a ¼-in. O.D. FEP reactor. Using a microsyringe, H_2O (77 μL, 43 μmol) was added to the reactor. Afterwards, an excess of SF_4 (0.540 g, 5.00 mmol) was distilled unto the white crystalline solid, which vigorously reacted at –80 °C. At room temperature, the sample separated into two phases with a yellow-white translucent liquid above liquid SF_4. Excess SF_4 was removed by vacuum at –50 °C leaving an off-white solid that was recrystallized in dichloromethane at –80 °C yielding clear, colourless crystals of $[C_6H_{12}N_4H]^+[HF_2]^-\cdot SF_4$. Raman spectra were recorded and crystals were characterized using X-ray crystallography.

Preparation of $[C_6H_{12}N_4]^+[H_2F_3]^-\cdot HF$. White crystalline HMTA (0.015 g, 0.11 mmol) was loaded into a ¼-in. O.D. FEP reactor in a nitrogen atmosphere dry-box. Using a microsyringe, H_2O (2 mg, 0.1 mmol) was added to the reactor. An excess of SF_4 (0.054 g, 50 μmol) was distilled into the reactor, reacting vigorously at –70 °C yielding a white solid suspended in liquid SF_4. Excess SF_4 was removed by vacuum at –44 °C followed by recrystallization in CH_2Cl_2 at –45 °C. Crystals of $[C_6H_{12}N_4]^+[H_2F_3]^-\cdot HF$ were characterized by Raman spectroscopy and X-ray crystallography.

Raman Spectroscopy. Raman spectra were recorded on a Bruker RFS 100 FT Raman spectrometer with a quartz beam splitter, a liquid-nitrogen cooled Ge detector, and R-496 temperature accessory. The actual usable Stokes range was 50 to 3500 cm^{-1}. The 1064-nm line of an Nd:YAG laser was used for excitation of the sample. The Raman spectra were recorded at –100 °C with a spectral resolution of 2 cm^{-1} using a laser power of 150 mW.

Crystallography. Crystals were mounted at low temperature under a stream of cold dry nitrogen as previously described.[24] The crystals were centered on a Bruker SMART APEX II diffractometer, controlled by the APEX2 Graphical User Interface software.[25] The program SADABS[26] was used for scaling of diffraction data, the application of a decay correction, and a multi-scan absorption correction. Structure solutions were obtained by direct methods. The programs SHELXS-97[27] and SHELXL-2014/6[28] were used for solution and refinement, respectively. During the refinement of the crystal structure of $[C_7H_{13}NH]^+F^-\cdot 3.5SF_4$ a disordered molecule was found at the 3 2 symmetry site that imposed an octahedral geometry. A refinement of SF_6 did not make chemical sense and did not produce a good model. Therefore, the electron density representing the disordered molecule was removed from the reflection files using the

SQUEEZE subroutine of PLATON[19] and the missing electron density matched that of SF_4. Modelling a disordered SF_4 gave the final R_1 factor of 0.0442, compared to 0.0417 for the squeezed structure. The crystallographic data can be obtained free of charge from The Cambridge Crystallographic Data Centre via www.ccdc.cam.ac.uk/data_request/cif.

ACKNOWLEDGEMENTS

We are thankful to the Natural Sciences and Engineering Research Council of Canada, the University of Lethbridge, and CFI for providing funding for this research. NK is thanking Alberta Government for an Indigenous Graduate Award.

ASSOCIATED CONTENT

Supporting Information

The Supporting Information is available free of charge on the ACS Publications website at DOI: XXX

X-ray crystallography data, thermal ellipsoid plots, and vibrational frequencies (PDF)

Accession Codes

CCDC 1994893 –1994898 contain the supplementary crystallographic data for this paper. These data can be obtained free of charge via www.ccdc.cam.ac.uk/data_request/cif, or by emailing data_request@ccdc.cam.ac.uk, or by contacting The Cambridge Crystallographic Data Centre, 12 Union Road, Cambridge, CB2 1EZ, UK; fax +44 1223 336033.

REFERENCES

(1) Dmowski, W. Introduction of Fluorine Using Sulfur Tetrafluoride and Analogs. In *Organo-Fluorine Compounds, Methods of Organic Chemistry, Houben-Weyl, Vol. E10a*; Baasner, B.; Hagemann, H.; Tatlow, J. C.; Eds.; Thieme: Stuttgart, **2000**, Ch. 8, pp. 321-431.

(2) Goettel, J.T.; Turnbull, D.; Gerken, M. A New Synthetic Route to Rhenium and Iodine Oxide Fluoride Anions: The Reaction between Oxoanions and Sulfur Tetrafluoride. *J. Fluorine Chem.* **2015**, *174,* 8-13.

(3) (a) Seel, F.; Detmer, O. Über Fluoro···onium-Verbindungen *Z. Anorg. Allg. Chem.* **1959**, *301*, 113-136; (b) Bartlett, N.; Robinson, P. L. Co-ordination Compounds Formed by Tetrafluorides of the Sulphur Sub-group. *J. Chem. Soc. A* **1961**, 3417-3425; (c) Gibler, D. D.; Adams, C. J.; Fischer, M.; Zalkin, A; Bartlett, N. Structural Studies of Trifluorosulfur(IV)yl, $[SF_3]^+$, Salts Including the Crystal Structure of $[SF_3]^+[BF_4]^-$. *Inorg. Chem.* **1972**, *11*, 2325-2329.

(4) (a) Tunder, R.; Siegel, B. The SF_5 Anion. *J. Inorg. Nucl. Chem.* **1963**, *25*, 1097-1098; (b) Christe, K. O.; Curtis, E. C.; Schack, C. J.; Pilippovich, D. Vibrational Spectra and Force Constants of the Square-Pyramidal Anions SF_5^-, SeF_5^-, TeF_5^-. *Inorg. Chem.* **1972**, *11,* 1679-1682; (c) Drullinger, L. F.; Griffiths, J. E. The SF_5^- anion: synthesis, structure, vibrational spectra and thermodynamic functions. *Spectrochim. Acta, Part A* **1971**, *27a*, 1793-1799; (d) Bittner, J.; Fuchs, J.; Seppelt, K. Die Kristallstruktur des SF_5^--Anions. *Z. Anorg. Allg. Chem.* **1988**, *557*, 182-190; (e) Clark, M.; Kellen-Yuen, C.; Robinson, K.; Zhang, H.; Yang, Z.-Y.; Madappat, K.; Fuller, J.; Atwood, J.; Thrasher, J. "Naked" SF_5^- anion: The crystal and molecular structure of $[Cs^+.(18\text{-crown-}6)_2][SF_5^-]$ *Eur. J. Solid State*

Inorg. Chem. **1992**, *29*, 809-833; (f) Matsumoto, K.; Haruki, Y.; Sawada, S.; Yamada, S.; Konno, T.; Hagiwara, R. Stabilization of SF_5^- with Glyme-Coordinated Alkali Metal Cations. *Inorg. Chem.* **2018**, *57*, 14882-14889.

(5) Goettel, J.T.; Chaudhary, P.; Mercier, H. P. A.; Hazendonk, P.; Gerken, M. $SF_4 \cdot N(C_2H_5)_3$: The First Conclusively Characterized SF_4 Adduct with an Organic Base. *Chem. Commun.* **2012**, *48*, 91209122.

(6) Chaudhary, P.; Goettel, J. T.; Mercier, H. P. A.; Sowlat-Hashjin, S.; Hazendonk, P.; Gerken, M. Lewis Acid Behavior of SF_4: Synthesis, Characterization and Computational Study of SF_4 Adducts with Pyridine and Pyridine-Derivatives. *Chem. Eur. J.* **2015**, *21*, 6247-6256.

(7) Goettel, J.T.; Gerken, M. Synthesis and Characterization of Adducts between Interactions between SF_4 and Oxygen-Bases: Example of O---S(IV) Chalcogen Bonding *Inorg. Chem.*, 2016, **55**, 12441-12450.

(8) (a) Nziko, V.D.P.N.; Scheiner, S. Chalcogen Bonding between Tetravalent SF_4 and Amines. *J. Phys. Chem. A* **2014**, *118*, 10849-10856; (b) Zierkiewicz, W.; Wysokiński, R.; Michalczyk, M.; Scheiner, S. Chalcogen bonding of two ligands to hypervalent YF_4 (Y = S, Se, Te, Po). *Phys. Chem. Chem. Phys.* **2019**, *21*, 20829-20839; (c) Franconetti, A.; Quinonero, D.; Frontera, A.; Resnati, G. Unexpected chalcogen bonds in tetravalent sulfur compounds. *Phys. Chem. Chem. Phys.* **2019**, *21*, 11313-11319.

(9) Goettel, J. T.; Kostiuk, N.; Gerken, M. Interactions between SF_4 and Fluoride: A Crystallographic Study of Solvolysis Products of SF_4·Nitrogen Base Adducts by HF. *Inorg. Chem.* **2016**, *55*, 7126-7134.

(10) (a) Vogel, L.; Wonner, P.; Huber, S. M. Chalcogen Bonding: An Overiew. *Angew. Chem. Int. Ed.* **2019**, *58*, 1880-1891; (b) Wang, W.; Zhu, H.; Feng, L.; Yu, Q.; Hao, J.; Zhu, R.; Wang, Y. Dual Chalcogen-Chalcogen Bonding Catalysis. *J. Am. Chem. Soc.* **2020**, *142*, 3117-3124; (c) Taylor, M. S. Anion recognition based on halogen, chalcogen, pnictogen and tetrel bonding. *Coord. Chem. Rev.* **2020**, *413*, article 213270.

(11) Iwaoka, M.; Takemoto, S.; Tomoda, S. Statistical and Theoretical Investigations on the Directionality of Nonbonded S···O Interactions. Implications for Molecular Design and Protein Engineering. *J. Am. Chem. Soc.* **2002**, *124*, 10613-10620.

(12) Laurence, C.; Gal, J. F. *Lewis Basicity and Affinity Scales*, John Wiley and Sons: Chichester, **2010**, Chapter 3.

(13) Laus, G.; Kahlenberg, V.; Wurst, K.; Lörting, T.; Schottenberger, H. Hydrogen bonding in the perhydrate and hydrates of 1,4-diazabicyclo[2.2.2]octane (DABCO). *Cryst. Eng. Comm.* **2008**, *10*, 1638.

(14) Nimmo, J. K.; Lucas, B. W. Solid-State Phase Transition in Triethylenediamine, $N(CH_2CH_2)_3N$. I. The Crystal Structure of Phase II at 298 K. *Acta Crystallogr. B*, **1976**, *B32*, 348.

(15) Cooney, A. P.; Crampton, M. R.; Golding, P. The Acid-Base Behaviour of Hexamine and its *N*-Acetyl Derivatives. *J. Chem. Soc., Perkin Trans. II*, **1986**, 835-839.

(16) Alvarez, S. A cartography of the van der Waals territories. *Dalton Trans.*, **2013**, *42*, 8617-8636.

(17) Goettel, J.T.; Kostiuk, N.; Gerken, M. The Solid-State Structure of SF_4: The Final Piece of the Puzzle. *Chem. Int. Ed.* **2013**, *52*, 8037-8040.

(18) Troyanov, S. I.; Morozov, I. V.; Kemnitz, E. Crystal Structures of Cesium Dihydrotrifluoride, CsH_2F_3. Refinement of the Crystal Structures of NMe_4HF_2 and $NMe_4H_2F_3$. *Z. Anorg. Allg. Chem.* **2005**, *631*, 1651.

(19) Van Der Sluis, P.; Spek, A. L. BYPASS: an effective method for the refinement of crystal structures containing disordered solvent regions. *Acta Crystallogr.A*, **1990**, *A46*, 194-201.

(20) Guzonas, D. A.; Irish, D. E. A Raman and infrared spectroscopic study of triethylenediamine (DABCO) and its protonated forms. *Can. J. Chem.* **1988**, *66,* 1249-1257.

(21) Paoletti, P.; Stern, J. H.; Vacca, A. Thermochemical Studies. XV. Thermodynamics of Protonation of Triethylenediamine, Triethylamine, Trimethylamine, and Ammonia in Aqueous Solution at 25°. *J. Phys. Chem.* **1965**, *69*, 3759-3762.

(22) Berney, C. V. SF_4: Vibrational spectra and structure of the solid. *J. Mol. Struct.* **1972**, *12*, 87-97.

(23) Bertie, J. E.; Solinas, M. Infrared and Raman spectra and the vibrational assignment of hexamethylenetetramine-h_{12} and -d_{12}. *J. Chem. Phys.* **1974**, *61*, 1666-1677.

(24) Gerken, M.; Dixon, D. A.: Schrobilgen, G. J. The OsO_4F^-, $OsO_4F_2^{2-}$, and $OsO_3F_3^-$ Anions and Their Study by Vibrational and NMR Spectroscopy and Density Functional Calculations; and the X-ray Crystal Structures of $[N(CH_3)_4][OsO_4F]$ and $[N(CH_3)_4][OsO_3F_3]$. *Inorg. Chem.* **2000**, *39*, 4244-4255.

(25) APEX 2; Bruker AXS Inc.; Madison, WI, **2006**.

(26) Sheldrick, G. M. *SADABS*, Version 2007/4, Bruker ACS Inc.; Madison, WI, **2007**.

(27) Sheldrick, G. M. SHELXTL97, University of Göttingen, Germany, **2008**.

(28) Sheldrick, G. M. SHELXTL-2014, University of Göttingen, Germany, **2014**.

Table of Contents Sypnosis and Graphic

Highly volatile and weakly Lewis acidic SF_4 forms adducts with DABCO ($C_6H_{12}N_2$) as well as HMTA ($C_6H_{12}N_4$) where SF_4 acts as a chalcogen bond donor. Whereas $C_6H_{12}N_2 \cdot 2SF_4$ forms N---S chalcogen bonds to two terminal SF_4 molecules, $C_6H_{12}N_4 \cdot 2SF_4$ crystallizes as a coordination polymer containing both terminal and bridging SF_4 molecules. In the presence of HF, the polycyclic amines DABCO, HMTA and quinuclidine form structures in which chalcogen bonds enable incorporation of large amounts of SF_4.